ACS Catalysis

Research Article

pubs.acs.org/acscatalysis

Ligand-Directed Regioselectivity in Amine−Imine Nickel-Catalyzed 1-Hexene Polymerization

Haibin Hu, Haiyang Gao,* Darui Chen, Guiliang Li, Yingxin Tan, Guodong Liang, Fangming Zhu, and Qing Wu*

PCFM Lab, GD HPPC Lab, DSAPM Lab, School of Chemistry and Chemical Engineering, Sun Yat-Sen University, Guangzhou 510275, China

Supporting Information

ABSTRACT: 1-Hexene polymerizations were carried out with amine−imine nickel complexes [(ArN═C(R^1)−(R^2R^3)CNHAr)-$NiBr_2$, **1a**, R^1 = R^2 = R^3 = Me, Ar = 2,6-$(iPr)_2C_6H_3$; **1b**, R^1 = R^2 = R^3 = Me, Ar = 2,6-$(Me)_2C_6H_3$; **2a**, R^1 = Me, R^2 = R^3 = H, Ar = 2,6-$(iPr)_2C_6H_3$; **3a**, R^1 = Me, R^2 = *t*Bu, R^3 = H, Ar = 2,6-$(iPr)_2C_6H_3$] in the presence of MMAO or Et_2AlCl. The ligand-directed regioselectivity involving insertion fashion and chain walking in amine−imine nickel-catalyzed 1-hexene polymerization is clearly observed. Catalyst **1a** with two methyl substituents on the bridging carbon can polymerize 1-hexene to afford semicrystalline "polyethylene" with long methylene sequence $(-(CH_2)_n-$, n = 40−74) via a combination of 90% selectivity of 2,1-insertion fashion and precise chain walking, whereas catalyst **3a** with a *tert*-butyl on the bridging carbon can polymerize 1-hexene in 80% selectivity of 1,2-insertion to produce amorphous polyolefin with predominant methyl branches through 2,6-enchainment.

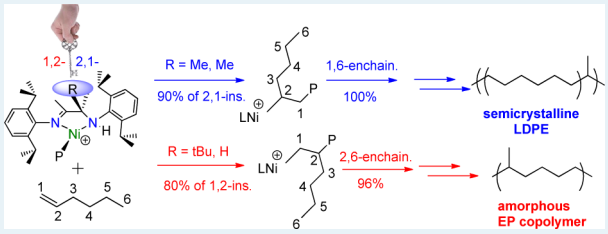

KEYWORDS: *1-hexene, nickel, chain walking, regioselectivity*

INTRODUCTION

Precise control of polyolefin microstructure by olefin coordination polymerization, including molecular weight and polydispersity, stereochemistry, and branch structure, is challenging and increasingly attractive because polyolefin architecture is closely related to mechanical and rheological properties.[1] Early transition metal catalysts have been developed that give precise control over polymer stereochemistry.[2] On the contrary, late transition metal catalysts such as α-diimine nickel and palladium show a distinguishing chain-walking mechanistic feature involving interaction between the metal center and β-H of the growing polymer chain.[3] In terms of α-olefins polymerization with α-diimine nickel and palladium catalysts, polymer branch structure including branching distribution and density is closely relative to the regioselectivity involving insertion fashion of α-olefin and chain-walking process.[4] In the case of abstraction of insertion from secondary carbon, 1,2-insertion of α-olefin and subsequent β-hydride elimination followed by metal migration up to the primary carbon atom can lead to 2,ω-enchainment to give methyl branch in the polymer chain, while 2,1-insertion of α-olefins can result in 1,ω-enchainment to give a linear polymer chain without branches. Amorphous poly(α-olefin)s are generally produced by late transition metal catalysts because of poor regioselectivity involving low selectivity of insertion fashion and uncontrolled chain walking.[5]

Currently, high selectivity of 1,2-insertion fashion of α-olefin have been achieved using symmetric α-diimine nickel and α-keto-β-diimine nickel catalysts at low temperature of −78 °C.[4e,6] Isotactic polypropylenes with mirror regioerrors were obtained because of restriction of chain walking at low temperature. One high regioselectivity example involving 1,2-insertion and chain walking is the aminobis(imino)-phosphorane nickel system, which can produce polyolefins with methyl branches at well-defined intervals through 2, ω-enchainment.[4a] In comparison with the 1,2-insertion fashion of α-olefin, high selectivity of 2,1-insertion is hardly achieved using nickel and palladium catalysts. The regioirregular poly(propylene) is usually produced in 2,1-insertion mode by Brookart-type α-diimine nickel catalysts because of occurrences of 1,3-enchainment and insertion from secondary carbon.[7] Modification of N-aryl substituents and ligand backbone of α-diimine nickel catalyst has been used to improve selectivity of 2,1-insertion.[4e,5g,8,9] The semicrystalline "polyethylenes" were recently generated from α-olefin monomers with the "sandwich" α-diimine nickel catalysts via a combination of regioselective 2,1-insertion and precision chain walking.[8] Our groups have also observed that the 2,1- insertion fashion occurs more frequently in the polymerizations of propylene and 1-hexene using an α-diimine nickel catalyst with a bulky camphyl backbone, and long methylene sequences are present in the polymers.[9]

A new type of amine−imine nickel catalyst was recently developed by our groups, and living polymerization of ethylene

Received: July 25, 2014
Revised: November 14, 2014
Published: November 17, 2014

   dx.doi.org/10.1021/cs501081a | ACS Catal. 2015, 5, 122−128

was achieved above room temperature to produce highly branched polymers.[10] Unlike α-diimine nickel catalyst, the amine−imine nickel catalyst bears two different coordinating functionalities (imine (sp^2) and amine (sp^3)),[11] which is anticipated to exhibit a distinctive influence on regioselectivity involving insertion fashion in the polymerization of α-olefin. Herein, we investigate this class of amine−imine nickel catalysts for polymerization of 1-hexene. Substituent groups on the carbon of amine group dominantly determine the selectivity of insertion fashion of 1-hexene. In combination with precise chain walking, amorphous polyolefin with a predominant methyl branch can be produced by catalyst **3a** with a *tert*-butyl group in 80% selectivity of 1,2-insertion, whereas "low density polyethylene" (LDPE) can be obtained by catalyst **1a** with two methyl substituents in 90% selectivity of 2,1-insertion. The high melting temperature of 107 °C for the semicrystalline polyolefin generated from 1-hexene monomer is also observed.

RESULTS AND DISCUSSION

Four amine−imine nickel complexes (see Scheme 1) were used for 1-hexene polymerization at various polymerization conditions (see Table 1) in the presence of MMAO or Et_2AlCl. Generally, amine−imine nickel complexes show relatively low catalytic activity for 1-hexene polymerization relative to α-diimine nickel analogue **4a** (entries 1−4 vs 7), which may arise from suppression of substantial steric bulk around nickel metal center for the coordination and stronger isomerization of 1-hexene.[4d,9] An observed tendency that increasing steric hindrance of amine−imine ligand results in a reducing polymerization activity and molecular weight also supports this claim. More notably, ligand structure significantly determines total branching density of the obtained polymer. A 4-fold increase in the total branching density of the polymer was observed when **3a** was used in the 1-hexene polymerization instead of **1a**.

Scheme 1. Structures of Amine−imine Nickel and α-Diimine Nickel Complexes

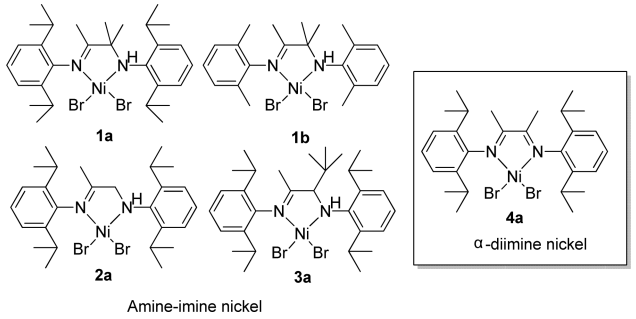

To gain deep insight into the definitive microstructure of polyolefin, the polymers obtained by various nickel catalysts were analyzed by ^{13}C NMR spectroscopy (Figure 1). Total branching density and the branching distribution are quantitatively calculated on the basis of previous resonance assignments and listed in Table 2.[4e,5n] The observed basic trend is that the branching density of the obtained polymers are lower than the theoretic value (166.7/1000C), which is a result of nickel migration on polymer chain. It is notable that only methyl, butyl, and long chain branches are present in the polymers obtained by amine−imine nickel catalysts. The absence of ethyl, propyl, and adjacent methyl branches (15−17 ppm) is indicative of no occurrence of insertion of 1-hexene into secondary Ni-alkyl bond.[4e,9a] Therefore, the 2,1-insertion of 1-hexene can always result in 1,6-enchainment to give methylene sequences $-(CH_2)_n-$ for amine−imine nickel catalysts.

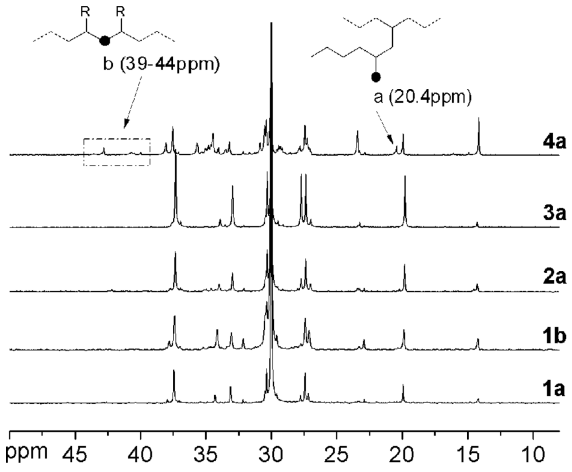

Figure 1. ^{13}C NMR spectra of the polymers produced by different nickel complexes/MMAO at 25 °C.

Table 1. 1-Hexene Polymerization Results by Different Nickel Catalysts[a]

entry	complex	cocatalyst	T (°C)	yield (g)	activity[b]	M_n[c] (kg/mol)	PDI[c]	BD[d] (/1000C)
1	**1a**	MMAO	25	0.149	0.93	20.5	1.49	34.8
2	**1b**	MMAO	25	0.323	2.02	25.9	1.60	43.8
3	**2a**	MMAO	25	0.333	2.08	39.9	1.76	60.9
4	**3a**	MMAO	25	0.177	1.11	31.8	1.23	132.2
5	**3a**	MMAO	15	0.063	0.39	16.0	1.20	135.4
6	**3a**	MMAO	50	0.240	1.50	58.2	1.46	106.1
7	**4a**	MMAO	25	0.960	6.00	198	1.72	85.8
8	**1a**	Et_2AlCl	0	0.035	0.22	5.2	1.40	17.1
9	**1a**	Et_2AlCl	25	0.063	0.39	7.0	1.41	25.5
10	**1a**	Et_2AlCl	50	0.148	0.92	14.9	1.49	32.9
11	**1a**	Et_2AlCl	75	0.090	0.56	9.6	1.66	41.3

[a]Conditions: 20 μmol Ni, Al/Ni = 200, [hexene]: 1.06 M; solvent: toluene, total volume: 30 mL, time: 8 h. [b]Activity (kg polymer/(mol Ni h)) was calculated by kg of polymer per mole of Ni catalyst per hour. [c]M_n (kg/mol) and PDI (M_w/M_n) were determined by high-temperature GPC against polystyrene standard. [d]Branching density, determined by ^{13}C NMR spectra.

dx.doi.org/10.1021/cs501081a | ACS Catal. 2015, 5, 122−128

Table 2. Branching Distribution and Characterization of the Polymers

			branching distribution (/1000C)[a]							
entry	cat.	T (°C)	Me	Et	Pr	Bu	Lg	BD (/1000C)	1,2/2,1-ins.[b]	T_m[c] (°C)
1	**1a**	25	30.2	0	0	0.9	3.7	34.8	0.21/0.79	87.8
2	**1b**	25	28.2	0	0	2.5	13.1	43.8	0.26/0.74	66.8
3	**2a**	25	46.7	0	0	7.3	5.0	60.9	0.36/0.64	58.7
4	**3a**	25	123.2	0	0	5.7	3.3	132.2	0.80/0.20	-[d]
5	**3a**	15	124.1	0	0	8.5	2.8	135.4	0.81/0.19	-[d]
6	**3a**	50	101.5	0	0	1.0	3.6	106.1	0.64/0.36	-[d]
7	**4a**	25	48.0	0	0	34.4	3.4	85.8	0.51/0.49	-[d]
8	**1a**	0	12.5	0	0	0.4	4.2	17.1	0.10/0.90	93.4, 107.2
9	**1a**	25	19.7	0	0	0.5	5.3	25.5	0.15/0.85	86.0, 98.2
10	**1a**	50	25.6	0	0	0.9	6.4	32.9	0.20/0.80	78.0, 90.3
11	**1a**	75	31.3	0	0	1.1	8.9	41.3	0.25/0.75	75.5, 89.2
12	**4a**[e]	0	30.9	0	0	66.8	1.8	99.5	0.60/0.40	-[d]
13	**4a**[e]	25	58.6	0	0	30.9	3.4	92.9	0.56/0.44	-[d]
14	**4a**[e]	50	61.1	0	0	20.1	6.2	87.4	0.52/0.48	-[d]
15	**4a**[e]	75	62.3	0	0	14.4	7.9	84.6	0.51/0.49	-[d]

[a]Branching density and distribution were calculated according to ^{13}C NMR spectra. Entries 1−7 were activated by MMAO, entries 8−15 were activated by Et_2AlCl. [b]Fraction of 1,2 and 2,1-insertion was calculated by equation: 2,1-insertion = (166.7-Br)/166.7 [c]Determined by DSC, T_m is peak value. All DSC traces of the polymers are seen in Figures S21−25. [d]Broad and weak endotherms, amorphous polymers. [e]Polymerization conditions (entries 12−15): 20 μmol Ni, Al(Et_2AlCl)/Ni = 200, [hexene]: 1.06 M, solvent: toluene, total volume: 30 mL, time: 8 h.

Scheme 2. Impossible Insertion Pathways of 1-Hexene and Chain Walking for Amine−Imine Nickel Catalysts

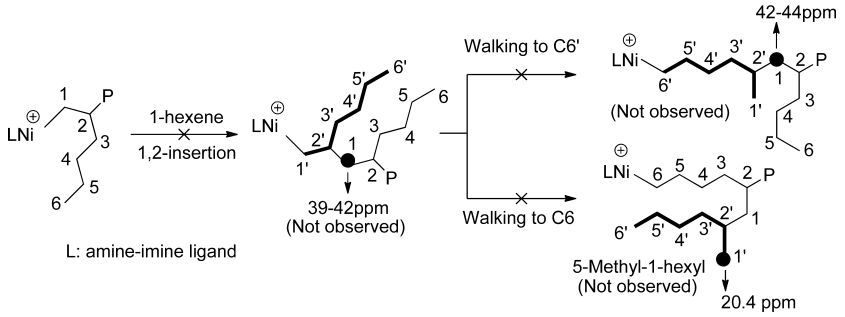

Scheme 3. Different Enchainment Pathways in 1-Hexene Polymerization Catalyzed by Amine−Imine Nickel 1a and 3a

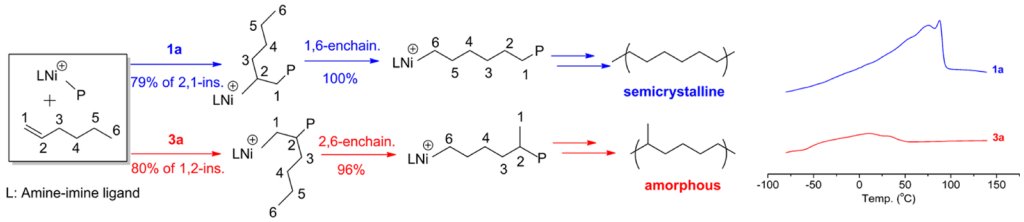

For comparison purposes, the spectrum of the polymer obtained by α-diimine nickel catalyst **4a**/MMAO (see Scheme 1) under the same polymerization conditions is shown and analyzed in Figure 1. A significant difference is the observation of only a small fraction of the butyl branch in the polymers obtained by amine−imine nickel catalysts relative to α-diimine nickel catalyst **4a**. Especially, only a trace of butyl branch (0.4−1.1/1000C) appears in the spectra of the polymers obtained by catalyst **1a** at 0−75 °C (entries 1, 8−11 in Table 2). According to the chain-walking mechanistic model, the butyl branch is generated from 1,2-insertion of 1-hexene without occurrence of chain walking.[4e] Therefore, two possible mechanisms should be responsible for a small fraction of the butyl branch of the polymers obtained by amine−imine nickel catalysts. One is a very small fraction of 1,2-insertion of 1-hexene, the other is a large transformation of 1,2-insertion to 2,6-enchainment by chain straightening to produce a short methyl branch. The fraction of 1,2- and 2,1-insertions can be predicted from the branching density on the basis of lack of occurrence of 1-hexene insertion in a secondary nickel−alkyl bond.[5q,r]

Calculation results in Table 2 clearly show that the actual fraction of 1,2-insertion is significantly dependent on nickel catalyst structure. Small fraction of 1,2-insertion of 1-hexene (0.21) is observed for **1a**/MMAO at 25 °C, whereas a large fraction of 1,2-insertion (0.80) is observed for **3a**/MMAO (entries 1 and 4−6 in Table 2). That is to say, a small fraction of the butyl branch in the polymers obtained by **1a**−**3a**/MMAO arises from different mechanisms. Small fraction of butyl branch is a result of small fraction of 1,2-insertion for **1a**/MMAO, whereas nearly full conversion of 1,2-insertion to 2,6-enchainment leads to very low fraction of butyl and high fraction of methyl branches for **3a**/MMAO in spite of ~80%

dx.doi.org/10.1021/cs501081a | ACS Catal. 2015, 5, 122−128

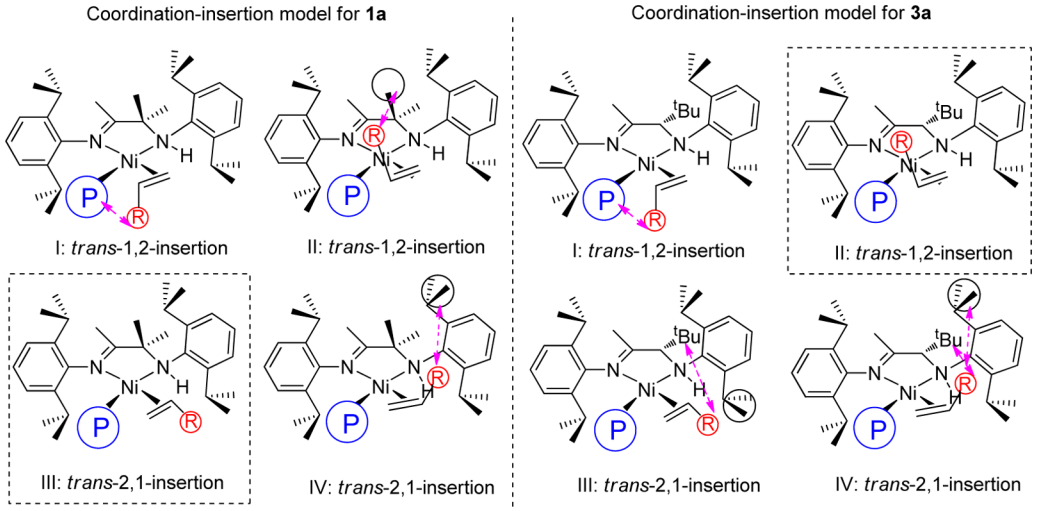

Figure 2. Proposed mechanistic model for coordination−insertion of 1-hexene.

Table 3. Polymerizations of α-Olefins with 1a/Et_2AlCl at 25 °C[a]

entry	monomer	yield (g)	activity[b]	M_n[c] (kg/mol)	PDI[c]	BD[d] (/1000C)	1,2/2,1-ins.	T_m[e] (°C)
16	propylene	0.280	7.0	8.5	1.52	78.8	0.24/0.76	[f]
9	1-hexene	0.063	0.39	7.0	1.41	25.5	0.15/0.85	86.0, 98.2
17	1-octene	0.336	0.35	32.0	1.61	17.2	0.14/0.86	95.0
18	1-dodecene	0.236	0.25	24.0	1.73	8.8	0.11/0.89	102.9
19	1-octadecene	0.153	0.16	16.0	1.59	5.2	0.09/0.91	103.1

[a]Conditions: 20 μmol Ni, Al/Ni = 200, 25 °C, solvent: toluene, total volume: 30 mL, propylene: 100 psig, [α-olefins]: 1.06 M; reaction time: 2 h for propylene, 8 h for 1-hexene, and 48 h for 1-octene, 1-dodecene and 1-octadecene. [b]Activity (kg PO/(mol Ni h)) was calculated by kg of PO per mole of Ni catalyst per hour. [c]M_n (kg/mol) and PDI (M_w/M_n) were determined by high temperature GPC against polystyrene standard. [d]Branching density, determined by ^{13}C NMR spectra. [e]Determined by DSC, T_m is peak value. All DSC traces of the polymers are seen in Figures S26−29. [f]Broad and weak endotherms, amorphous polymers.

selectivity of 1,2-insertion. The influence of temperature on branching density of the polymer also shows that 1,2-insertion of 1-hexene is predominant for catalyst **3a**/MMAO (entries 4, 5 in Table 2). The more steady support comes from ^{13}C NMR spectrum of the polymer obtained by **3a**/MMAO. There are no existences of α,α-methylene carbons and 5-methyl-1-hexyl branch in the ^{13}C NMR spectrum of the polymer obtained by **3a**/MMAO, while these signals can be clearly observed in the ^{13}C NMR spectrum of the polymer obtained by α-diimine nickel catalyst **4a**/MMAO (Figure 1). This result proves that nearly full transformation of 1,2-insertion to 2,6-enchainment occurs in amine−imine nickel catalyst **3a**, which is different to α-diimine nickel catalyst **4a**/MMAO (see Scheme 2).

The above ^{13}C NMR analyses show that catalyst **1a** and **3a** exhibit high but opposite regioselectivity in 1-hexene polymerization by a combination of the high selectivity of insertion fashion and precise chain walking. Different enchainment pathways in these two amine−imine nickel-catalyzed 1-hexene polymerizations can be briefly illustrated in Scheme 3 (for detailed mechanistic pathways, see Scheme S1 in Supporting Information (SI)). For catalyst **1a**/MMAO, 79% of all insertions is 2,1-insertion fraction in the 1-hexene polymerization at 25 °C, and all 2,1-insertions completely transfer to 1,6-enchainment to produce a semicrystalline polymer (low density polyethylene) with a melting point of 87.8 °C. For catalyst **3a**, 80% of all insertions is 1,2-insertion fraction at 25 °C, and 96% of 1,2-insertion undergoes chain straightening (2,6-enchainment) to produce an amorphous polymer (ethylene-propylene copolymer analogue) with a T_g of −55 °C.

Obviously, the distinctive regioselectivities in 1-hexene polymerization by **1a**/MMAO and **3a**/MMAO come from different ligand substituents. In the square-planar resting state for olefin polymerization, the polymer chain and olefin monomer are considered to coordinate to the Ni(II) center besides the auxiliary bidentate [N, N] ligand.[4b,c,11a] Unlike the symmetric α-diimine nickel system, the amine−imine nickel system bearing hybrid N functionalities can lead to selective geometrical isomerism in square planar configuration because of unique microenvironment around nickel center (see Figure S20 in SI). Chen has presented that *trans*-form is more stable than *cis*-form with respect to the steric place in the ethylene polymerization on the basis of calculation analysis.[11] The bulky polymer growing chain is *cis* to the imine functionality, while the small ethylene monomer is seated *cis* to the amine. It is reasonably deduced that the same *trans*-form is favorable for 1-hexene polymerization with amine−imine nickel catalyst.

On the basis of the coordination−insertion mechanism model, four possible model structures necessary for insertion in each case are shown in Figure 2. The steric interactions significantly determine insertion fashion of 1-hexene, as previously reported by Brookhart.[4e] For catalyst **1a** with two methyl substituents on the ligand backbone, the alignment necessary for 1,2-insertion always results in interaction of the C-4 substituent of hexene with growing polymer chain (**I**) or the methyl on backbone (**II**). Therefore, the structure (**III**, left) by *trans* 2,1-insertion of 1-hexene is favorable for catalyst **1a**. In contrast, for catalyst **3a** with a *tert*-butyl substituent on backbone, the alignment necessary for 2,1-insertion always

dx.doi.org/10.1021/cs501081a | ACS Catal. 2015, 5, 122−128

results in interaction of the C-4 substituent of hexene with a *tert*-butyl on backbone (**III**) or an ortho isopropyl group (**IV**). The structure (**II**, right) by *trans* 1,2-insertion of 1-hexene seems to be sound for catalyst **3a**. These analyses suggest that ligand substitution plays a decisive role in the shift of insertion mode of 1-hexene for amine−imine nickel catalyst. Catalyst **2a** without substituent on the carbon shows relatively poor selectivity of 1-hexene insertion (entry 3). Reducing the steric hindrance of the N-aryl substituents by substituting of *o*-methyl groups for *o*-isopropyl groups results in reducing 2,1-insertion fraction (entries 1 vs 2). These results further support the proposed mechanistic study for 1-hexene polymerization using amine−imine nickel catalysts.

Polymerizations of α-olefins including propylene, 1-octene, 1-decene, and 1-octadecene were also performed with **1a**/Et_2AlCl at 25 °C to evaluate the influence of monomer chain length on the selectivity of insertion fashion, and the results are listed in Table 3. Except for propylene (Figure S26), other α-olefin monomers can be polymerized to produce semicrystalline polyethylenes with low branching densities (see Figure S27−29 in SI). With an increase in the monomer chain length, selectivity of 2,1-insertion increases and melting temperature of the corresponding polymer increases basically despite the presence of a longer branch on the polymer chain. This result suggests that interaction of substituent of α-olefins with ligand substitution has an important influence on insertion fashion of monomer, proving the proposed mechanistic model from another point of view.

Although ligand-directed regioselectivity in 1-hexene polymerization is dominant, polymerization parameters including cocatalyst type and reaction temperature have also an influence on regioselectivity. Complex **1a** is selected to further study these effects of polymerization parameters. When Et_2AlCl compound was used as an activator instead of MMAO for polymerization of 1-hexene (entry 1 vs 9 in Table 1), the polymer with lower branching density but larger fraction of long branches was obtained. This result indicates that the **1a**/Et_2AlCl system shows a higher selectivity of 2,1-insertion and stronger chain-walking performance than the **1a**/MMAO system.[5r] A similar observation has been reported by our groups in α-diimine nickel-catalyzed α-olefin polymerization.[5q,9b] The influence of cocatalyst type on regioselectivity in 1-hexene polymerization can be assigned to the nature of the interaction between nickel metal complex and activator. On the basis of the reported α-diimine nickel active species such as ion-pair and halogen bridge models, organoaluminate anion formed from Et_2AlCl is smaller than that generated from MMAO, enabling a closer interaction with nickel center, which could explain the higher selectivity of 2,1-insertion fashion.[12] Besides, higher Lewis acidity of Et_2AlCl may have an influence of insertion mode of α-olefin.[5q,13]

The microstructure characterizations of the polymers obtained by **1a**/Et_2AlCl system in the temperature range from 0 to 75 °C were determined by ^{13}C NMR spectra to probe the effect of polymerization temperature (entries 8−11). A basic tendency is that branching density and methyl fraction as well as long branches fraction decrease with reducing temperature. In contrast, branching density increases with reducing temperature for the α-diimine nickel **4a**/Et_2AlCl system (entries 12−15). Figure 3 also clearly shows the opposite trend on the temperature dependence of the selectivity of 2,1-insertion for both catalytic systems. This result further supports that 2,1-insertion is favorable for amine-

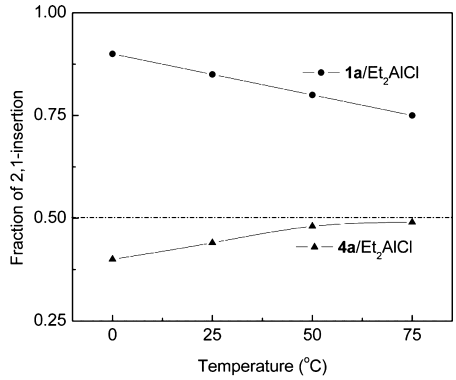

Figure 3. Dependence of 2,1-insertion fraction on temperature using **1a**/Et_2AlCl and **4a**/Et_2AlCl.

nickel **1a**/Et_2AlCl system at low temperature, and α-diimine nickel **4a**/Et_2AlCl has a poor selectivity in insertion mode of 1-hexene.

It is interesting to note that the highest selectivity (90%) of 2,1-insertion of 1-hexene can be achieved and fully transfers to 1,6-enchainment at 0 °C using **1a**/Et_2AlCl (entry 8). To the best of our knowledge, this is one of the extremely rare reports on high regioselectivity involving 2,1-insertion mode and precise chain walking in α-olefin polymerization with late transition metal catalyst.[8] The polymer with low branching density as well as high melting temperature (T_m = 107 °C) and 35% crystallinity can be produced at 0 °C. The melting temperature of 107 °C is much higher than previously reported values of the polyolefin generated from 1-hexene monomer obtained by other nickel catalysts.[4e,5g,8,9]

It is known that the branch structure of the polyolefin can be also reflected by the thermal analysis. To further support NMR analyses, differential scanning calorimetry (DSC) analyses were conducted at a rate of 10 °C/min and recorded at second heating curves to examine the thermal behavior of the polymers. Figure 4 shows DSC thermograms of the polymers

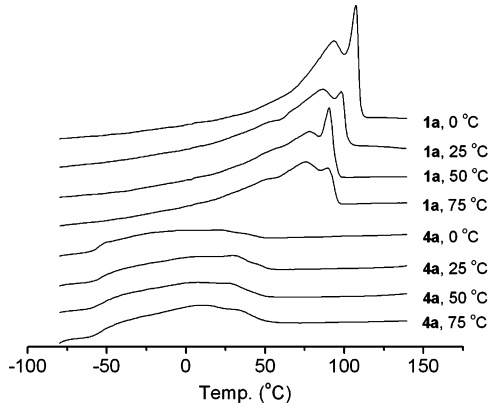

Figure 4. DSC curves of the polymers produced by **1a**/Et_2AlCl and **4a**/Et_2AlCl at different temperatures.

obtained by **1a**/Et_2AlCl and **4a**/Et_2AlCl at various temperatures. Obvious melting endotherms of the polymers obtained by **1a**/Et_2AlCl can be observed. Indistinct T_m and broad endotherm are the results of the irregularity in placing methyl branches along the backbone and methylene sequences with small number of branches.[9a] The observed trend is that the melting temperature (T_m) of polymer product increases with a

dx.doi.org/10.1021/cs501081a | ACS Catal. 2015, 5, 122−128

reducing polymerization temperature for **1a**/Et_2AlCl. Differently, the polymers produced by **4a**/Et_2AlCl at various temperatures show broad and weak melting endotherms extending to a much lower temperature (−50 °C) in DSC curves. This is a result of poor regioselectivity and well consistent with ^{13}C NMR analyses. Wide-angle X-ray diffraction (WAXD) analyses (Figure 5) further prove that the T_m comes

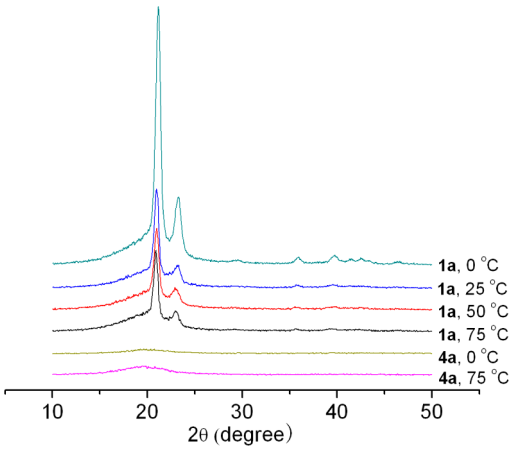

Figure 5. WAXD spectra of the polymers produced by **1a**/Et_2AlCl and **4a**/Et_2AlCl at different temperatures.

from the presence of the methylene sequences in the polyolefin. Two characteristic crystalline peaks at 21.3° and 23.6° were observed for the four polymer samples by catalyst **1a**/Et_2AlCl, which can be assigned to 110 and 200 planes of linear polyethylene. That is to say, the polymer materials obtained by **1a**/Et_2AlCl seemingly are low density polyethylene (LDPE) with predominant methyl branch. However, no obvious diffraction signals were detected for the polyolefins produced by α-diimine nickel **4a**/Et_2AlCl because of their amorphous morphologies.

According to endotherm transitions of branched modeling PE reported by Wagener,[14] a branched modeling PE with 39 methylenes between two adjacent methyl branches show melting temperature of 92 °C[14b] while a branched modeling PE with 74 methylenes between two adjacent butyl branches show melting temperature of 104 °C.[14c] Therefore, it is reasonably deduced that the polymers obtained by **1a**/Et_2AlCl should contain long polymethylene sequences with 40−74 carbons. Over seven successive 1,6-enchainments of 1-hexene can solely occur in polymerization using catalyst **1a**/Et_2AlCl. This result is consistent with 2,1-insertion fraction calculated by ^{13}C NMR analysis.

CONCLUSIONS

In summary, we report that ligand-directed regioselectivity in 1-hexene polymerization using amine−imine nickel catalysts bearing hybrid nitrogen functionalities. Substituents on the carbon of amine group are located at a strategic place for high selectivity of insertion fashion of 1-hexene. Shift of 1,2-insertion to 2,1-insertion of 1-hexene can be facilely achieved by tuning the substituents on the carbon adjacent to amine moiety. A high regioselectivity up to 90% involving high 2,1-insertion selectivity of 1-hexene and sequential precise chain walking can be achieved by catalyst **1a**/Et_2AlCl at 0 °C. The obtained semicrystalline polymer obtained shows an obvious melting endotherm up to 107 °C because of the presence of long methylene sequences ($-(CH_2)_n-$, n = 40−74). High regioselectivity involving 1,2-insertion selectivity of 80% and sequential precise 2,6-enchainment (96%) can be also achieved by **3a**/MMAO to afford amorphous polyolefin with predominant methyl branches. Our study provides a novel access to facilitating the development of late transition metal catalysts with better control of regiochemistry by tuning different coordinating functionalities of N atom donor. Further optimization of electronic effect in amine−imine frameworks will enable improvements in regioselectivity and monodispersity in α-olefin polymerization.

EXPERIMENTAL SECTION

General Considerations. All manipulations involving air- and moisture-sensitive compounds were carried out under an atmosphere of dried and purified nitrogen with standard vacuum-line, Schlenk, or glovebox techniques.

Materials. The amine−imine nickel complexes used in this article were prepared according to literature procedures.[10a,b] Dichloromethane was distilled from P_2O_5 under nitrogen, and toluene from Na/K alloy. Modified methylaluminoxane (MMAO, 7 wt % Al in heptane) was purchased from Akzo-Nobel and used as received. Diethylaluminum chloride (Et_2AlCl, 1.0 M in hexane) was purchased from Acros. 1-Hexene, 1-octene, 1-dodecene, and 1-octadecene were purchased from Alfa Aesar Chemical, dried over CaH_2, and distilled under nitrogen before use.

Characterization. The ^{13}C NMR data of polyolefin samples were obtained on a Varian Mercury-Plus 500 MHz spectrometer at 110 °C, o-$C_6D_4Cl_2$ solution using 30 ppm for main chain of PE as a reference. Branching content and distribution, as well as the fraction of 2,1-insertion were calculated according to the literature.[4e,5q,r] The molecular weight and the molecular weight distribution of the polyolefins were determined on PL-220 instrument at 150 °C, and 1,2,4-trichlorobenzene was employed as the eluent at a flow rate of 1.0 mL/min, and data were treated using narrow polystyrene standards. Differential scanning calorimetry (DSC) analysis was conducted with a PerkinElmer DSC-7 system in a heating or cooling rate of 10 °C/min and was recorded at second heating or cooling curves from −100 to 140 °C. Wide-angle X-ray diffraction (WAXD) was performed on an X-ray diffractometer (D/max 2200 vpc, Japan) using Cu Kα 1 (λ = 0.154056 nm) as radiation source.

Polymerization of α-Olefins. In a typical procedure, a round-bottom Schlenk flask with stirring bar was heated 3 h to 150 °C under vacuum and then cooled to room temperature. A proper amount of freshly distilled α-olefin was introduced into the flask, which contained the required amount of activator and toluene. Polymerization was started by injecting the catalyst solution (20 μmol, 2 mL CH_2Cl_2) into the reactor, and the total volume of solvent was kept 30 mL. After reaction for the desired time, the polymerizations were terminated by adding 200 mL of the acidic ethanol (ethanol−HCl, 95:5). The precipitated polymer was collected and treated by filtering, washing with ethanol several times, and then drying in vacuum at 60 °C to a constant weight.

Polymerization of Propylene. A mechanically stirred 100 mL Parr reactor was heated to 150 °C for 3 h under vacuum and then cooled to room temperature. The autoclave was pressurized to 100 psig of propylene and vented three times. The autoclave was then charged with 28 mL of a solution of Et_2AlCl, and then the nickel complex solution (2 mL) was

dx.doi.org/10.1021/cs501081a | ACS Catal. 2015, 5, 122−128

charged into the autoclave. The ethylene pressure was raised to 100 psig, and the reaction was carried out for 2 h. Polymerization was terminated by addition of acidic ethanol after releasing propylene pressure. The resulting precipitated polymers were collected and treated by filtering, washing with ethanol several times, and drying under vacuum at 60 °C to a constant weight.

■ ASSOCIATED CONTENT

Supporting Information

The following file is available free of charge on the ACS Publications website at DOI: 10.1021/cs501081a.

Detailed NMR spectra of the polymers and assignments, GPC and DSC curves of the polymers, molecular structure of **1a** and **3a**, and detail mechanistic model involving insertion fashion and chain walking in 1-hexene polymerization (PDF)

■ AUTHOR INFORMATION

Corresponding Authors

*E-mail: gaohy@mail.sysu.edu.cn (H.G.).
*E-mail: ceswuq@mail.sysu.edu.cn (Q.W.).

Notes

The authors declare no competing financial interest.

■ ACKNOWLEDGMENTS

Financial support by the National Natural Science Foundation of China (NSFC) (21174164, 51173209, 21274167, and 21374134), and Technology Innovation Project of Educational Commission of Guangdong Province of China (2013KJCX0002) are gratefully acknowledged.

■ REFERENCES

(1) (a) Lodge, T. P. *Macromol. Chem. Phys.* **2003**, *204*, 265−273. (b) Mülhaupt, R. *Macromol. Chem. Phys.* **2003**, *204*, 289−327.

(2) (a) Britovsek, G. J. P.; Gibson, V. C.; Wass, D. F. *Angew. Chem., Int. Ed.* **1999**, *38*, 428−447. (b) Coates, G. W. *Chem. Rev.* **2000**, *100*, 1223−1252. (c) Gibson, V. C.; Spitzmesser, S. K. *Chem. Rev.* **2003**, *103*, 283−315.

(3) (a) Ittel, S. D.; Johnson, L. K.; Brookhart, M. *Chem. Rev.* **2000**, *100*, 1169−1204. (b) Mecking, S. *Coord. Chem. Rev.* **2000**, *203*, 325−351. (c) Mecking, S. *Angew. Chem., Int. Ed.* **2001**, *40*, 534−540. (d) Camacho, D. H.; Guan, Z. *Chem. Commun.* **2010**, *46*, 7879−7893. (e) Liu, F. S.; Hu, H. B.; Xu, Y.; Guo, L. H.; Zai, S. B.; Song, K. M.; Gao, H. Y.; Zhang, L.; Zhu, F. M.; Wu, Q. *Macromolecules* **2009**, *42*, 7789−7796. (f) Guo, L. H.; Gao, H. Y.; Guan, Q. R.; Hu, H. B.; Deng, J. A.; Liu, J.; Liu, F. S.; Wu, Q. *Organometallics* **2012**, *31*, 6054−6062.

(4) (a) Mohring, V. M.; Fink, G. *Angew. Chem., Int. Ed.* **1985**, *24*, 1001−1003. (b) Schubbe, R.; Angermund, K.; Fink, G.; Goddard, R. *Macromol. Chem. Phys.* **1995**, *196*, 467−468. (c) Killian, C. M.; Tempel, D. J.; Johnson, L. K.; Brookhart, M. *J. Am. Chem. Soc.* **1996**, *118*, 11664−11665. (d) Gottfried, A. C.; Brookhart, M. *Macromolecules* **2003**, *36*, 3085−3100. (e) McCord, E. F.; McLain, S. J.; Nelson, L. T. J.; Ittel, S. D.; Tempel, D.; Killian, C. M.; Johnson, L. K.; Brookhart, M. *Macromolecules* **2007**, *40*, 410−420. (f) Subramanyam, U.; Rajamohanan, P. R.; Sivaram, S. *Polymer* **2004**, *45*, 4063−4076.

(5) (a) Bomfim, J. A. S.; Dias, M. L.; Filgueiras, C. A. L.; Peruch, F.; Deffieux, A. *Catal. Today* **2008**, *133−135*, 879−885. (b) Merna, J.; Cihlar, J.; Kucera, M.; Deffieux, A.; Cramail, H. *Eur. Polym. J.* **2005**, *41*, 303−312. (c) Subramanyam, U.; Sivaram, S. *J. Polym. Sci., Part A: Polym. Chem.* **2007**, *45*, 1093−1100. (d) Peruch, F.; Cramail, H.; Deffieux, A. *Macromolecules* **1999**, *32*, 7977−7983. (e) Suzuki, N.; Yu, J.; Masubuchi, Y.; Horiuchi, A.; Wakatsuki, Y. *J. Polym. Sci., Part A: Polym. Chem.* **2003**, *41*, 293−302. (f) Ye, Z.; Feng, W.; Zhu, S.; Yu, Q. *Macromol. Rapid Commun.* **2006**, *27*, 871−876. (g) Camacho, D. H.; Guan, Z. *Macromolecules* **2005**, *38*, 2544−2546. (h) Cherian, A. E.; Rose, J. M.; Lobkovsky, E. B.; Coates, G. W. *J. Am. Chem. Soc.* **2005**, *127*, 13770−13771. (i) Rose, J. M.; Cherian, A. E.; Lee, J. H.; Archer, L. A.; Coates, G. W.; Fetters, L. J. *Macromolecules* **2007**, *40*, 6807−6813. (j) Rose, J. M.; Deplace, F.; Lynd, N. A.; Wang, Z.; Hotta, A.; Lobkovsky, E. B.; Kramer, E. J.; Coates, G. W. *Macromolecules* **2008**, *41*, 9548−9555. (k) Rose, J. M.; Cherian, A. E.; Coates, G. W. *J. Am. Chem. Soc.* **2006**, *128*, 4186−4187. (l) Peleška, J.; Hoštálek, Z.; Hasalíková, D.; Merna, J. *Polymer* **2011**, *52*, 275−281. (m) Azoulay, J. D.; Schneider, Y.; Galland, G. B.; Bazan, G. C. *Chem. Commun.* **2009**, 6177−6179. (n) Azoulay, J. D.; Bazan, G. C.; Galland, G. B. *Macromolecules* **2010**, *43*, 2794−2800. (o) Leone, G.; Losio, S.; Piovani, D.; Sommazzi, A.; Ricci, G. *Polym. Chem.* **2012**, *3*, 1987−1990. (p) Guo, L.; Gao, H.; Li, L.; Wu, Q. *Macromol. Chem. Phys.* **2011**, *212*, 2029−2035. (q) Gao, H.; Liu, X.; Tang, Y.; Pan, J.; Wu, Q. *Polym. Chem.* **2011**, *2*, 1398−1403. (r) Gao, H.; Pan, J.; Guo, L.; Xiao, D.; Wu, Q. *Polymer* **2011**, *52*, 130−137.

(6) Azoulay, J. D.; Gao, H.; Koretz, Z. A.; Kehr, G.; Erker, G.; Shimizu, F.; Galland, G. B.; Bazan, G. C. *Macromolecules* **2012**, *45*, 4487−4493.

(7) (a) McCord, E. F.; McLain, S. J.; Nelson, L. T. J.; Arthur, S. D.; Coughlin, E. B.; Ittel, S. D.; Johnson, L. K.; Tempel, D.; Killian, C. M.; Brookhart, M. *Macromolecules* **2001**, *34*, 362−371. (b) Pellecchia, C.; Zambelli, A. *Macromol. Rapid Commun.* **1996**, *17*, 333−338. (c) Pellecchia, C.; Zambelli, A.; Oliva, L.; Pappalardo, D. *Macromolecules* **1996**, *29*, 6990−6993.

(8) Vaidya, T.; Klimovica, K.; LaPointe, A. M.; Keresztes, I.; Lobkovsky, E. B.; Daugulis, O.; Coates, G. W. *J. Am. Chem. Soc.* **2014**, *136*, 7213−7216.

(9) (a) Liu, F.; Gao, H.; Hu, Z.; Hu, H.; Zhu, F.; Wu, Q. *J. Polym. Sci., Part A: Polym. Chem.* **2012**, *50*, 3859−3866. (b) Liu, J.; Chen, D.; Wu, H.; Xiao, Z.; Gao, H.; Zhu, F.; Wu, Q. *Macromolecules* **2014**, *47*, 3325−3331.

(10) (a) Gao, H.; Hu, H.; Zhu, F.; Wu, Q. *Chem. Commun.* **2012**, *48*, 3312−3314. (b) Hu, H.; Zhang, L.; Gao, H.; Zhu, F.; Wu, Q. *Chem.—Eur. J.* **2014**, *20*, 3225−3233. (c) Zai, S. B.; Liu, F. S.; Gao, H. Y.; Li, C.; Zhou, G. Y.; Cheng, S.; Guo, L. H.; Zhang, L.; Zhu, F. M.; Wu, Q. *Chem. Commun.* **2010**, *46*, 4321−4323. (d) Zai, S.; Gao, H.; Huang, Z.; Hu, H.; Wu, H.; Wu, Q. *ACS Catal.* **2012**, *2*, 433−440.

(11) (a) Yang, F.; Chen, Y.; Lin, Y.; Yu, K.; Liu, Y.; Wang, Y.; Liu, S.; Chen, J. *Dalton Trans.* **2009**, 1243−1250. (b) Lin, Y.; Yu, K.; Huang, S.; Liu, Y.; Wang, Y.; Liu, S.; Chen, J. *Dalton Trans.* **2009**, 9058−9067. (c) Yang, F.; Wang, Y.; Chang, M.; Yu, K.; Huang, S.; Liu, Y.; Wang, Y.; Liu, S.; Chen, J. *Inorg. Chem.* **2009**, *48*, 7639−7644.

(12) (a) de Souza, R. F.; Simon, L. C.; do Carmo, M.; Alves, M. *J. Catal.* **2003**, *214*, 165−168. (b) Fusco, R.; Longo, L.; Masi, F.; Garbassi, F. *Macromol. Rapid Commun.* **2000**, *21*, 458−463.

(13) Caroline, G.; de Souza, R. F.; de Souza, K. B.-G. *Appl. Catal. A: General* **2007**, *325*, 87−90.

(14) (a) Baughman, T. W.; Sworen, J. C.; Wagener, K. B. *Macromolecules* **2006**, *39*, 5028−5036. (b) Inci, B.; Lieberwirth, I.; Steffen, W.; Mezger, M.; Graf, R.; Landfester, K.; Wagener, K. B. *Macromolecules* **2012**, *45*, 3367−3376. (c) Inci, B.; Wagener, K. B. *J. Am. Chem. Soc.* **2011**, *133*, 11872−11875. (d) Rojas, G.; Wagener, K. B. *Macromolecules* **2009**, *42*, 1934−1947. (e) Smith, J. A.; Brzezinska, K. R.; Valenti, D. J.; Wagener, K. B. *Macromolecules* **2000**, *33*, 3781−3794. (f) Zuluaga, F.; Inci, B.; Nozue, Y.; Hosoda, S.; Wagener, K. B. *Macromolecules* **2009**, *42*, 4953−4955.